

# Intelligent Real-Time Fitness Observation System Using IoT and Deep Learning

Kasi Venkata kiran\*1, T. Srinivasa Rao 2

<sup>1,2</sup>Department of Computer Science and Engineering, GITAM University, Vizag, AP, India. Emails: <a href="mailto:kasi.kvk@gmail.com">kasi.kvk@gmail.com</a>; <a href="mailto:sthamada@gitam.edu">sthamada@gitam.edu</a>

#### **Abstract**

The widespread adoption of smart healthcare monitoring systems is on the rise due to IoT-powered handy medical devices. Now the integration of IoT and the deep learning cutting-edge the healthcare activity is transforming patient care by shifting from traditional in-person consultations to telemedicine, aiding in disease prevention. In the context of safeguarding athletes from severe, life dangerous conditions like hurts, wounds and injuries during competitions and training time, continuous instantaneous observing of physical indicators show off fundamental. This study introduces a real-time health observing system based on deep learning and IoT. The system relies on vesture examination machines to collect essential health data and leverages deep learning algorithms in the direction of obtain valuable insights. Specifically, this research focuses on Sanda players as the case study. Deep learning algorithms enable doctors to accurately assess the athletes' health and prescribe appropriate treatments, even from remote locations. The proposed system's performance is rigorously tested through cross-validation using various statistical performance metrics, demonstrating its effectiveness in diagnosing serious diseases such as brain tumors, heart conditions, and cancer. Key performance metrics including precision, recall, AUC, and F1 are worked to calculate the system's efficiency.

**Keywords:** Deep neural network, Deep learning network, Diseases, Healthcare system, Internet of things.

# 1. Introduction

Health is a fundamental aspect of human life, often defined as the absence of illness and the presence of good physical and mental well-being. Across societies, increasing attention is being directed towards healthcare systems, which are rapidly incorporating technology. The COVID-19 pandemic, in particular, has had a profound economic impact globally, accelerating the shift toward smart healthcare systems. These systems enable remote monitoring to curb disease transmission and provide swift, cost-effective treatments. Integrating IoT-enabled healthcare systems with machine learning has emerged as a promising solution. Advances in sensing technology, data processing, spectrum use, and artificial intelligence have made these solutions more efficient, thanks to microelectronics that have produced compact, affordable medical sensors, revolutionizing healthcare services. Healthcare systems today focus on both symptomatic and preventive treatments, with an increasing emphasis on early disease detection and effective treatment for chronic conditions. Consequently, the growth of nationwide health observing systems has enhanced a significant tendency. In telemedicine, IoT systems in addition the machine learning algorithms are gaining attention for their role in remotely monitoring individuals and enabling accurate diagnoses. There is growing demand for real-time healthcare approaches that remain capable of energy-effective and cost-effective monitoring vital signs. However, traditional wireless communication in healthcare faces challenges such as high costs and radiation exposure, whereas real-time health monitoring systems offer flexible communication options suits to designed for various conditions. For instance, household data can be transmitted via local wireless networks, while portable devices enable communication outdoors. Machine learning systems are employed to figure informed options based on whether an individual is indoors or outdoors. IoT-enabled healthcare systems increasingly utilize deep learning algorithms, particularly in sports, where these technologies assist in tracking athletes' health. Wearable technology embedded in clothing can intelligently monitor metrics such as pace, respiration, muscle usage, and heart rate. These innovations significantly benefit athletes by ensuring balanced exercise routines. However, IoT devices produces infinite amounts of unstructured telemedicine data with complex correlations and

the outlier data, necessitating deep learning methods [1] to extract valuable information and minimize data redundancy.

The role of these algorithms in eliminating outliers and reducing redundancies is crucial, as they ensure that only refined, relevant information reaches healthcare management systems for decisionmaking. In sports informatics, where time-sensitive applications are common, deep learning's ability to process raw data with multiple hidden layers makes it indispensable for extracting high-level features. Given the large, heterogeneous datasets generated in sports, deep neural networks can autonomously identify essential features without human intervention, making them valuable tools for processing unstructured data [2]. This study proposes an IoT-enabled realistic smart health observing system that utilizes the DL algorithms to monitor players. Portable tiny medical devices are used to portray physiological indicators, and DL algorithms are applied to extract actionable insights. The study focuses on Sanda athletes, with results based on their health status. The proposed system collects vital signs and transmits the data remotely representing future analysis. Doctors use this data to identify diseases, evaluate athletes' specifications, and prescribe appropriate treatments. The system's performance has been rigorously tested and has proven to be an efficient tool in health observation. Key aids of this investigation include: the development of a real-time health observation system using portable tiny medical devices are attached to the Sanda athletes to obtain health data, the deployment of clothing devices for continuous observing through the wireless network and use the deep leaning technique to get the optimized results. The system achieves accurate predictions during data transmission, storage, and analysis. The paper proceeds by detailing the system design in Section 2, outlining the DL architecture in Section 3, presenting experimental results are in Section 4, and concluding with comments and ideas representing further investigation in the Section 5.

### 2. Existing Methods

The most relevant studies in this area are summarized below. In the article [3], Obaidat et al. assess WBAN concert by evaluating the packets reception ratio in conjunction with strength indicator of Receiver Signal, using efficiency benchmarking for resource management. In the article [4], an adaptive TPC system was introduced for energy conservation in image-based health observing systems, utilizing real-time monitoring datasets. Their findings indicate that while the dynamic quality of radio links significantly impacts energy and reliability, their proposed adaptive TPC method prioritizes energy savings over reliability, which may not be ideal for healthcare applications. Given the sensitive nature of medical data, a reliable, sustainable, and delay-tolerant approach is necessary. Cheour et al. give an summary of routing protocols and energy managing strategies for both global and local systems [5]. R. Miao Yu. [6] proposed an ass energy consumption method representing medical imaging using pill endoscopy in cutting-edge BANs, where energy consumption is controlled by regulating transmission power adaptively. However, their research does not consider key parameters like reliability and latency, nor does it examine the performance using the received signal strength indicator (RSSI). Healthcare platforms, particularly those operating at 2.4 GHz, require analysis of static on-body channel characterization and link quality [7]. Energy efficiency is central to developing sustainable and smart healthcare systems, with TPC-driven techniques being key contributors [8][9]. Xiao et al. developed innovative TCP algorithms for energy-saving in BANs, utilizing extensive experimental setups [10]. Sodhro et al. propose power-efficient strategies for media transmission, including a novel framework for heart attack patients, though they do not consider TPCbased strategies [11]. A specialized technique for telemedicine systems, optimizing medical-OoS, could prove beneficial in various medical scenarios [12]. Adaptive energy-saving mechanisms show more advantages over traditional methods, particularly in medical applications, and have been tested on real-time datasets with dynamic transmission power levels [13]. Won et al. introduced a TPCbased energy-saving approach for wireless networks [14], while the concept of power-awareness and battery duration expansion for vesture devices through media communication in WBSNs has been highlighted as essential [15]. Chenfu et al. introduced an energy-saving mechanism focusing only on internal circuitry transmission, without addressing other parts of the transceiver [16]. Evaluated using Monte Carlo simulations, this framework is reported to save significant power at suitable PLR levels owing to its self-adaptive environment. Y. H. Ugur et al. proposed a scheduling strategy using a game hierarchy for resource allocation in wireless communications [17]. An innovative framework described in [18] combines four different methods and algorithms to jointly adjust TPC and the duty cycle of BSNs for energy optimization. Additionally, two distinct systems for IoT-based smart cities were presented in [19]. The first system optimizes energy consumption by dynamically adjusting

sing

bandwidth and power in small nodes, while the second focuses on controlling transmission delays. Tanwar et al. [20] developed an IoT-based intelligent home system for elderly citizens, addressing power-efficient communication. Researchers worldwide have also emphasized concerns related to data processing related to health, security, and the enhancement of smart home mechanisation systems for IoT [21]–[27].

#### 3. Proposed System

The proposed system for real-time health observation system is designed to track the healthiness of Sanda players utilizing IoT-integrated habiliment devices. These devices, attached to the athletes, continuously gather data, which is then transmitted to a server via a relay network. This setup allows for ongoing monitoring and evaluation of the players health. As illustrated in Fig. 1, the approach is composed of three key components: wearable IoT devices, wireless relay network for transmission, and a server for physical d condition assessment and supervision. The figures shows the detailed explanation of all devices.

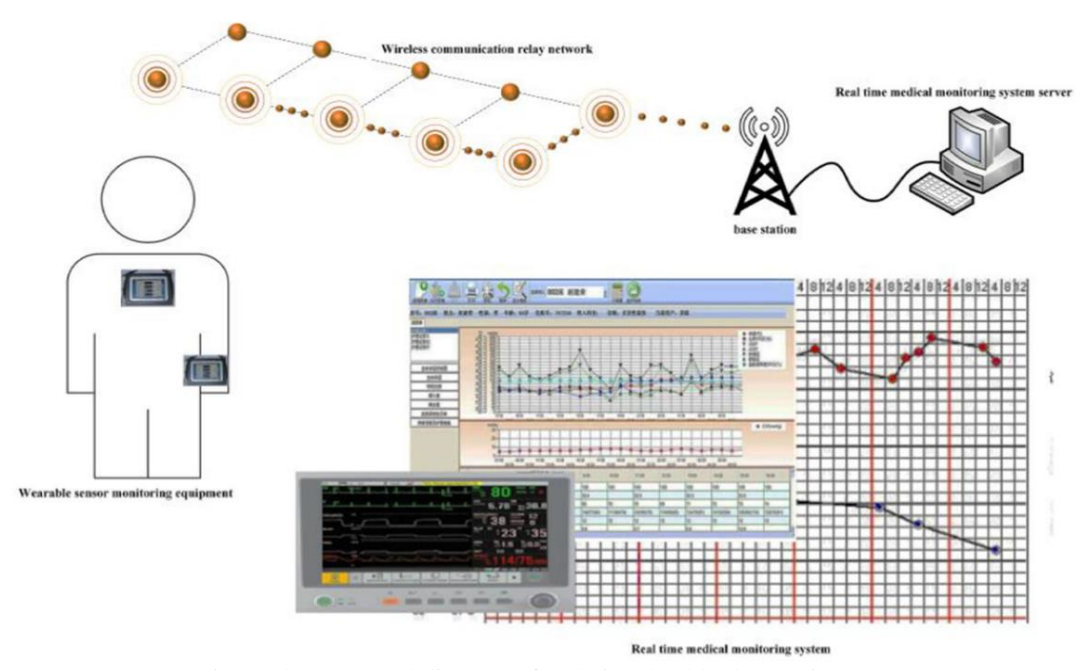


Fig. 1 The structural diagram of real-time health observation system [28]

## 3.1 Wearable IoT devices

IoT-enabled detecting devices gather various data types from athletes, such as pulse, blood pressure, body temperature, blood glucose, heart rate, and dynamic reduction observation. Currently, these devices, combined with DL algorithms, are worked to track numerous physiological signs and monitor athletes' health for chronic conditions. The collected data is transmitted regularly to a health measurement and observing server, enabling doctors to track real-time information and issue early warnings in case of abnormalities, achieving early detection and prevention [29].

To ensure accurate measurement and timely transmission of physical signals, wearable devices are utilized. This system contains two kinds of sensor units: one sensor for chest band unit and another sensor for wrist band unit. These modules are designed with plug-in functionality, allowing them to simultaneously interpret data from various sensors, such as 3D accelerometers, ECG sensors, and oxygen saturation sensors. Data communication is facilitated through a universal radio sensor structure section, which connects towards operatives or wireless systems, as illustrated in Figure 2. Both the chest strap and wrist strap sensor modules regularly send measurement data through this wireless frame module. The sensor modules are designed with a standard interface, enabling the integration of different sensors based on individual needs for monitoring various physical metrics. These Apparatus support many sensing segments by a flexible basis, forming a BAN abbreviated by Body Area Network by the common radio set module [30, 31].



# 3.2. Wireless relay network

By the adverse effects of emission on the body of humans, relay-enabled transreceiver is deemed more appropriate, as it relies on low-range interaction, reducing the need for high transmission power. The development of an effective IoT-enabled radio sensor transmission system is crucial. In this research, we propose the design of a less-power radio relay system, augmented by utilizing TinyOS [31] for the sensor operating system. TinyOS employs data fragmentation and retransmission techniques, improving both data transmission efficacy and accuracy. Every wearable detecting and observing devices communicate data towards the relay system effectively, minimizing the consumption of power. Additionally, the implementation of a transmission through the communication protocol that utilizes rapid initialization and time window system substantially enhances communication efficacy while reducing apparatus energy utilization. The improved processing flow of the sensor device operating system is illustrated in Figure 3.

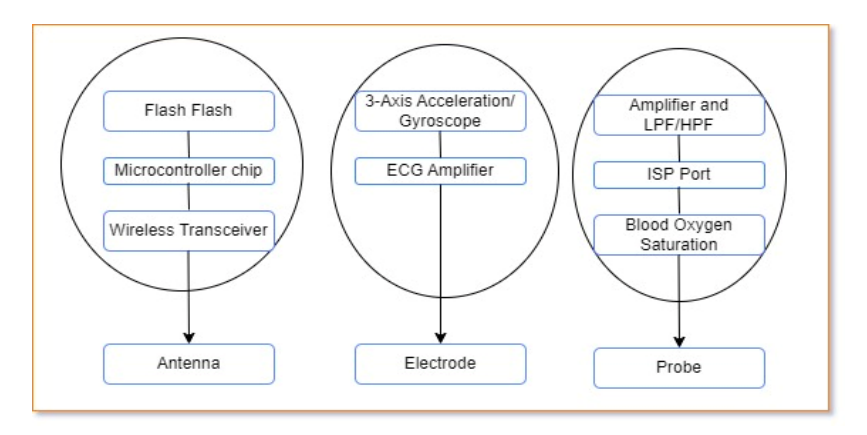


Figure 2. Architectural diagram of a generic wireless sensor system, adaptive from [32]

### 3.3 Medical Health observing system

This system is capable of continuously tracking the health of multiple individuals. It automatically collects and compiles health condition details on a everyday basis from each person's records. By integrating the expertise of various connoisseurs and medical specialists, the system provides comprehensive monitoring, early diagnoses, and timely warnings about potential health issues. Key features of the system include online health checkup monitoring, tendency investigation of health conditions, early warning alerts, detailed health reports, health care recommendations, custom-made health observing, emergency watching, and several additional purposeful modules.

#### 4. Architectural Model of Deep Neural Network

In this part, we present the pattern and model of intended model. The design of the representation is illustrated in Figure 4, which includes various key components. Each of these components is discussed in detail below:

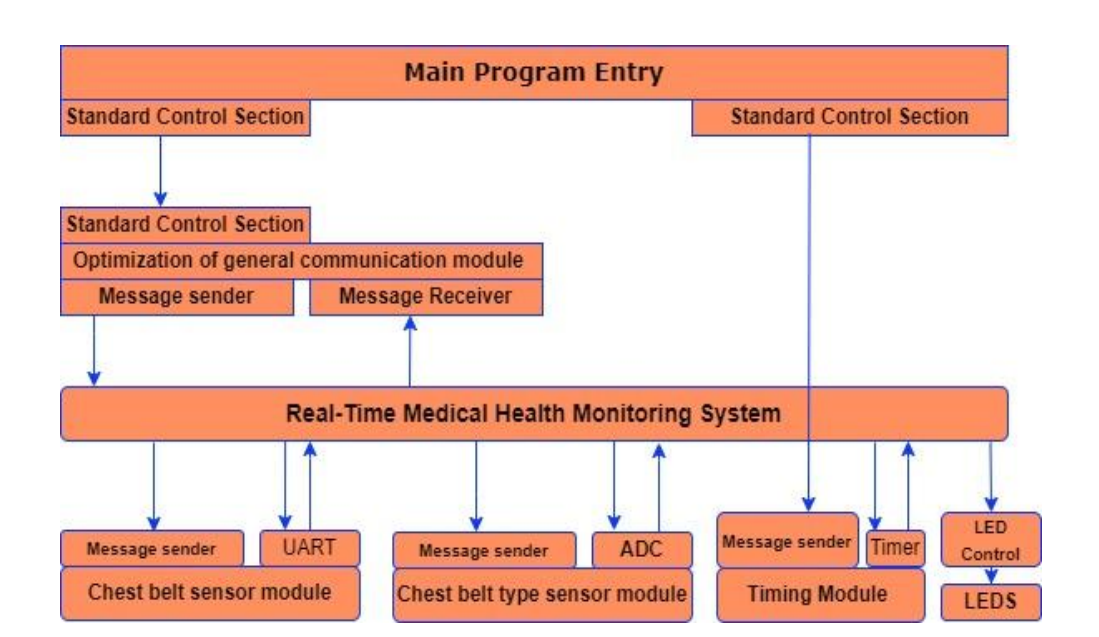


Figure. 3 Architectural diagram TinyOS adaptive from [32]

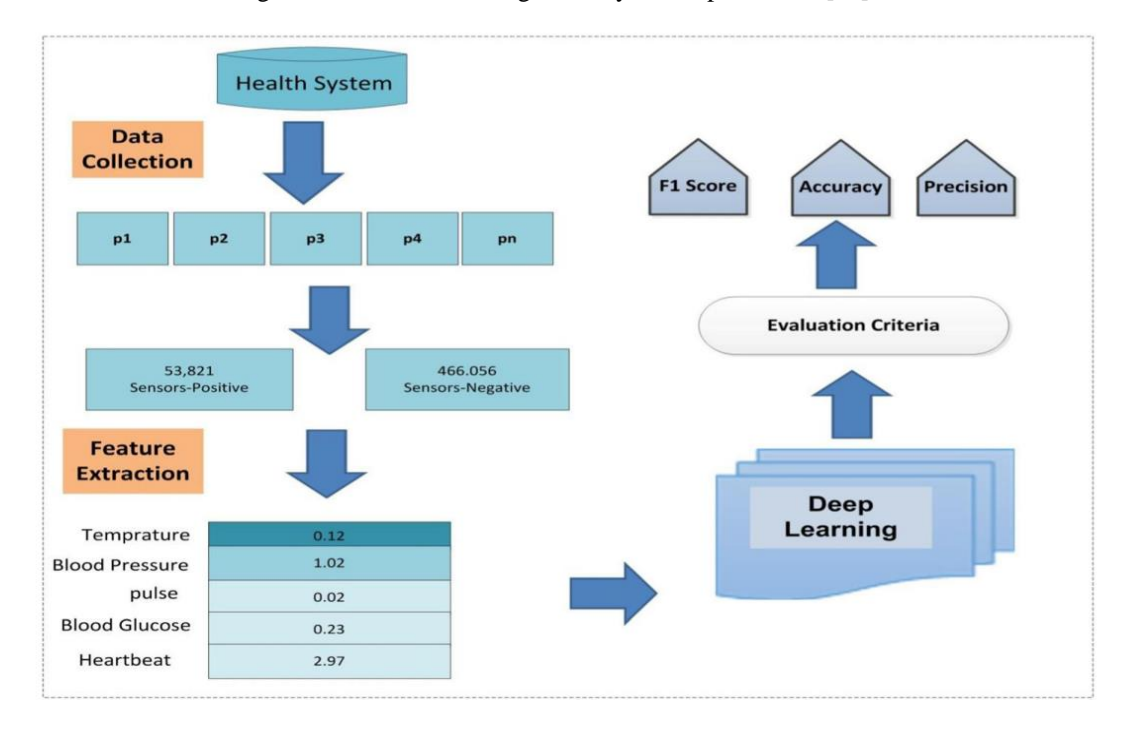


Figure. 4 Complete architectural diagram of Deep neural network

#### 4.1 DNN Model

DNN is a subdivision of the machine learning within the part of artificial intelligence, modelled after the functioning of the human brain furthermore their processes. The deep neural network consists of three primary components: the input layers, output layers as well as several hidden layers, being depicted in Figure 5. Various hidden layers entertainment a vital role in the DNN model, actively contributing to the learning process. Incorporating more hidden layers during model training can potentially enhance the model's efficiency.

$$y_{a} = f(B_{a} + \sum_{L=1}^{m} x_{b} W_{b}^{a}$$
 (1)

Conversely, strengthening the amount of hidden layers can also lead to higher computational costs, increased model complexity, and the risk of overfitting [13, 33]. The mathematical expression of the DNN model is presented in Equation (1).

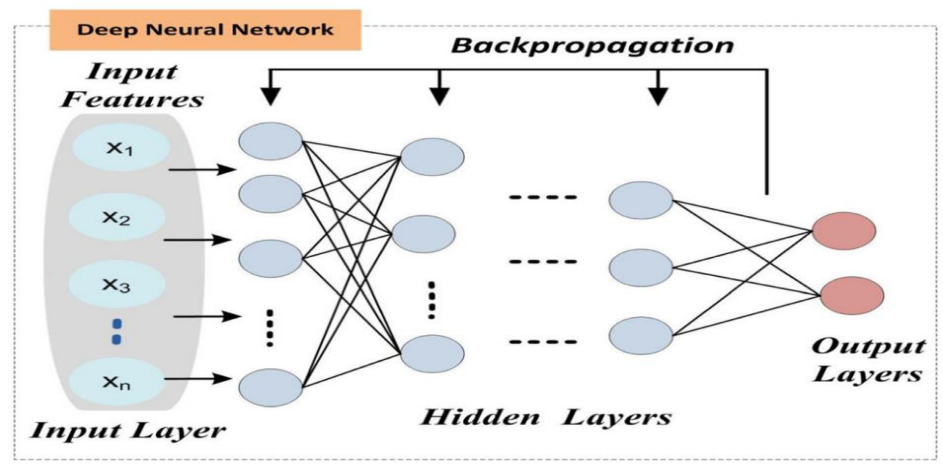


Fig. 5 Layered operational diagram of Deep neural network.

The  $y_a$  represent output at layer a, B represents bias value, the  $w_a^b$  representing the weights used at a layer a by a neuron b. The  $X_a^b$  represents input feature and f represent nonlinear activation Tanh function. It can be calculated using Eq. (2).

$$f(i) = \frac{e^i}{1 + e^i} \tag{2}$$

There are various justifications why we opted the DNN model instead of more conventional machine learning algorithms. First of all, single-layer processing is the foundation of most conventional algorithms, which makes them unsuitable for managing complicated datasets with significant nonlinearity. Second, the best features for precise predictions must be manually extracted using traditional machine learning techniques, which call for engineering knowledge or human experience. But DNNs are better suited to tackle these issues for the reason that of their inherent ability to automatically study and extract the features from data.

#### 4.2 Data Reduction and Denoising algorithm

Both dimensionality reduction and denoising are often necessary steps in preprocessing to increase the efficiency of machine learning models or to extract clearer insights from data. We use Principal Component Analysis (PCA) [34] is a usually applied technique for data reduction and denoising. PCA essentially involves mapping data from its original interstellar towards a new space while preserving the core information and eliminating redundant components. The method functions by identifying a group of rectangular conversion stands popular the actual interplanetary and constructing a fresh coordinate approach popular the transformed space, guided by the covariance of the original data [35]. This process effectively reduces dimensionality by projecting N-dimensional features onto a lower-dimensional space, thereby minimizing noise. Let X samples of data  $x = \{x^1, x^2, \dots, x^N\}$ ; each test says N-dimensional features like  $x_i = \{x_i^1, x_i^2, \dots, x_i^N\}$ ;

**Step 1:** Initially find mean 
$$X^1$$
 of the  $i^{th}$  feature to attain a latest sample:  $\bar{x}_i = \{x_i^1 - \bar{x}_1, x_i^2 - \bar{x}_2, \dots, x_i^N - \bar{x}_N\}$  (3)

**Step 2:** Next calculate the covariance of  $\bar{x}_i$  to acquire matrix C:

$$C = \begin{bmatrix} COV(x_1, x_1) & COV(x_1, x_2) \cdots \cdots & COV(x_1, x_N) \\ COV(x_2, x_1) & COV(x_2, x_2) \cdots \cdots & COV(x_2, x_N) \\ COV(x_N, x_1) & COV(x_N, x_2) \cdots \cdots & COV(x_N, x_N) \end{bmatrix}$$
(4)

Together with the  $COV(x_1, x_2)$  is to obtain the covariance of  $x_1$  as well as  $x_2$ , the formulary is:

$$cov(x_1, x_2) = \frac{\sum_{M}^{i=1} (x_i^1 - \bar{x}) (x_i^2 - \bar{x})}{M - 1}$$
 (5)

Step 3: Calculate the eigenvector that is  $u=u_1, u_2, \ldots, u_N$  as well as eigenvalue  $\lambda$  by the C matrix; Then, the filter is base as the k eigen vectors, and it shows the latest eigen-vectors to attain reductional dimensionality information after Y.

$$Y = \begin{bmatrix} y_i^1 \\ y_i^2 \\ y_i^2 \\ \vdots \\ y_i^N \end{bmatrix} \begin{bmatrix} u_1^T ( x_i^1, x_i^2, \dots, x_i^N)^T \\ u_2^T ( x_i^1, x_i^2, \dots, x_i^N)^T \\ \vdots & \vdots & \vdots \\ u_2^T ( x_i^1, x_i^2, \dots, x_i^N)^T \end{bmatrix}$$
(6)

**Step 4:** At finally we choose maximum eigen values of the k values.

## 4.3 Optimization Algorithm

In logistic regression and linear regression tasks, the Gradient Descent (GD) algorithm [36] is frequently used. It finds the minimum value iteratively, moving in the direction of the steepest gradient with each step to efficiently approach the minimum value. The following formula represents the Gradient Descent algorithm mathematically.

$$\theta = \theta - \eta \Delta J(\theta) \tag{7}$$

In the equation, g and h represent the representation parameters and the learning rate, correspondingly.  $(I(\theta))$  and  $\Delta I(\theta)$  denote the lossy and gradient functions, correspondingly. These are updated with each sample set used, significantly accelerating the model's update rate. The expression for the Stochastic Gradient Descent (SGD) approach is represented by.

$$\theta = \theta - \eta \Delta J(\theta; x_i, y_i) \tag{8}$$

Selecting the right learning rate is essential when using the gradient descent method. An excessive learning rate can make the model oscillate instead of converging to the best solution. On the other hand, a low learning rate will cause the convergence to lag and increase the number of iterations needed. A lower learning rate ought to be associated with a larger gradient in theory [37, 38]. Another gradient-based optimization algorithm that deals with this is called Adagrad; it does this by dynamically changing the learning rate. The accumulated square of earlier gradients is used to adjust the learning rate. Equations (9) and (10) give the formulas for changing the learning rate and the answer.

$$g_{i,t} = g_{i,t-1} + \eta \Delta J(\theta_{i,t})^2$$
 (9)

$$g_{i,t} = g_{i,t-1} + \eta \Delta J(\theta_{i,t})^{2}$$

$$\theta_{i,j} = \theta_{i,t-1} - \frac{\eta}{\sqrt{\theta_{i,t} + \epsilon}} \Delta J(\theta_{i,t})$$
(9)

 $J(\theta_{i,t})$  represents the gradient, t represents iteration and i is parameter, the  $g_{i,t}$  represents the summation of squared gradients of the  $i^{th}$  parameter in the earlier t iterations, furthermore  $\epsilon$  is tracing value that avoids become zero by the denominator. Hence, then the learning rate is various according to the gradient. But the given formula shown  $\eta / \sqrt{\theta_{i,t} + \epsilon}$  causes results in a continuous reduction of

the learning rate as the denominator increases, causing the learning rate to approach zero in the later stages of the iteration. Towards address the least fatigue issue encountered with Adagrad [39, 40], AdaDelta introduces the attenuation coefficient ρ to reduce an impact of long-term accumulated gradients on the current training process. This coefficient helps to mitigate the influence of past gradients, ensuring that recent gradient information has a more significant effect on updates. AdaDelta updates the solution for  $g_{i,t}$  using the following formula:

$$g_{i,t} = wg_{i,t-1} + (1-w)\Delta J \big(\theta_{i,j}\big)^2 \,. \label{eq:gitting}$$

$$v(t) = \rho_1 V(t-1) + (1-\rho_1) \Delta J(\theta)$$

$$g_t = \rho_2 g_{t-1} + (1-p_2) \Delta J(\theta^2)$$

$$V(t) = v(t) / (1-\rho_1) \Delta J(\theta^2)$$
(11)

$$\theta_{t} = \theta_{t-1} - \frac{\eta}{\sqrt{\widetilde{g_{t} + \epsilon}}} \widetilde{v(t)}$$
 (12)

parameter momentum is represented by V(t) and the constant parameters like  $q_1$  and  $q_2$ . During this training process, parameters are updated more independently, which results in quicker training and greater stability. Adam and NADAM optimizers are frequently employed due to their ability to leverage the usage of prior algorithms. Although a proposed model implements Adam and Nadam optimization techniques, they negatively impact the model's overall efficiency and performance.

### 5. Experiment and Results

Wearable sensor devices are employed representing real-time observing and crowd sampling in this experimentation. As Fig. illustrates. 6. Throughout the experiment, multiple crucial markers can be determined and monitored concurrently thanks to the equipment.

#### 5.1 Data measurement

The wristband sensor's absorption levels of two different light types—red and infrared—are used to calculate the blood  $O_2$  dissemination data. Based on the ratio of these lights on the hardware surface, this measurement is computed. The wristband sensing device measures blood oxygen saturation, photoplethysmographic pulse wave signals (PPG), and heart rate information. These metrics are composed the data packet size is 5 bytes per second.

#### 5.2 Data transmission measures

In order to measures the data transmissions, it has collected the abiliment sensor apparatus node first locates the closest sensor node of the wireless relay network. After deciding on the best route and also operating within a predetermined area and the wireless transmission relay sensor node sends the data to the base station. A Radio Frequency transceiver chip, one battery, and a microcontroller accomplish the wireless device relay sensor node. It can be transmitted the calculated acceleration, ECG data, and blood O<sub>2</sub> saturation to the ground station linked to the wireless radio server medical health observation system. Following the adoption of TinyOS's component programming mode, Figure 6 demonstrates the optimized component configuration, emphasizing elements like "blood oxygen saturation" and "ECGC.". Red-coloured components have undergone special modifications to enhance efficiency and wireless relay sensor network transmission. This routing strategy addresses low energy consumption, maintains network configuration stability, and guarantees high-efficiency transmission.

## 5.3 Test results

Whenever perform the initial performance tests exercising wrist and chest buckle sensing devices, that approach can be efficiently monitor an individual's situation via a wireless radio transmission network. Using low-power wireless relay nodes ensures effective caliculated data transmission from wearable recognizing and sensing devices to the medical healthiness monitoring system. Wireless relay nodes outperform pipelined routing networks or single network topologies in terms of communication performance because they automatically find the shortest path. Figure 7 illustrates the data transmission packet arrangement for the attached sensor device. Each data packet contains measurement values for acceleration, blood oxygen saturation, and ECG.

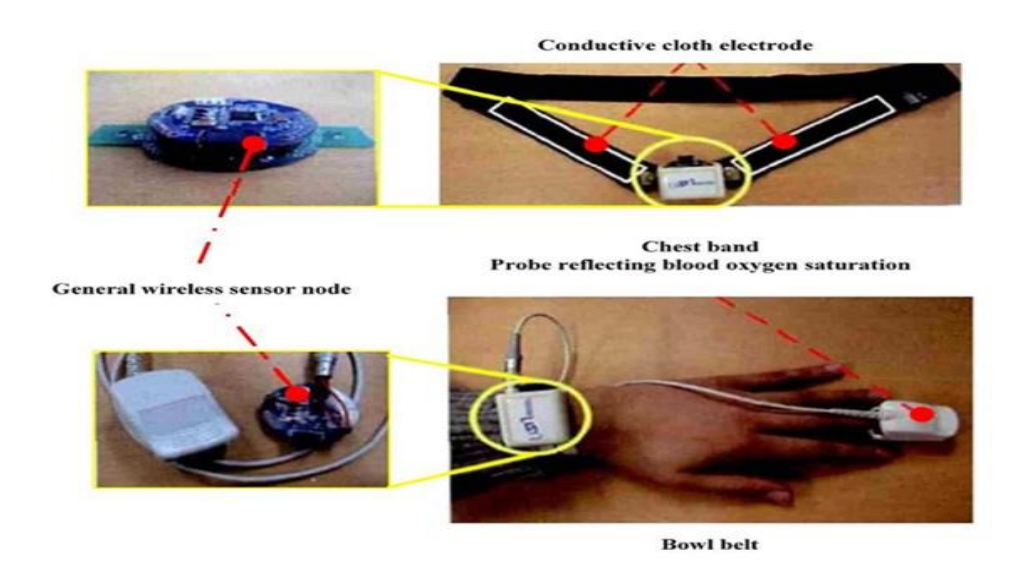


Fig. 6 Structural diagrams of different wireless relay node

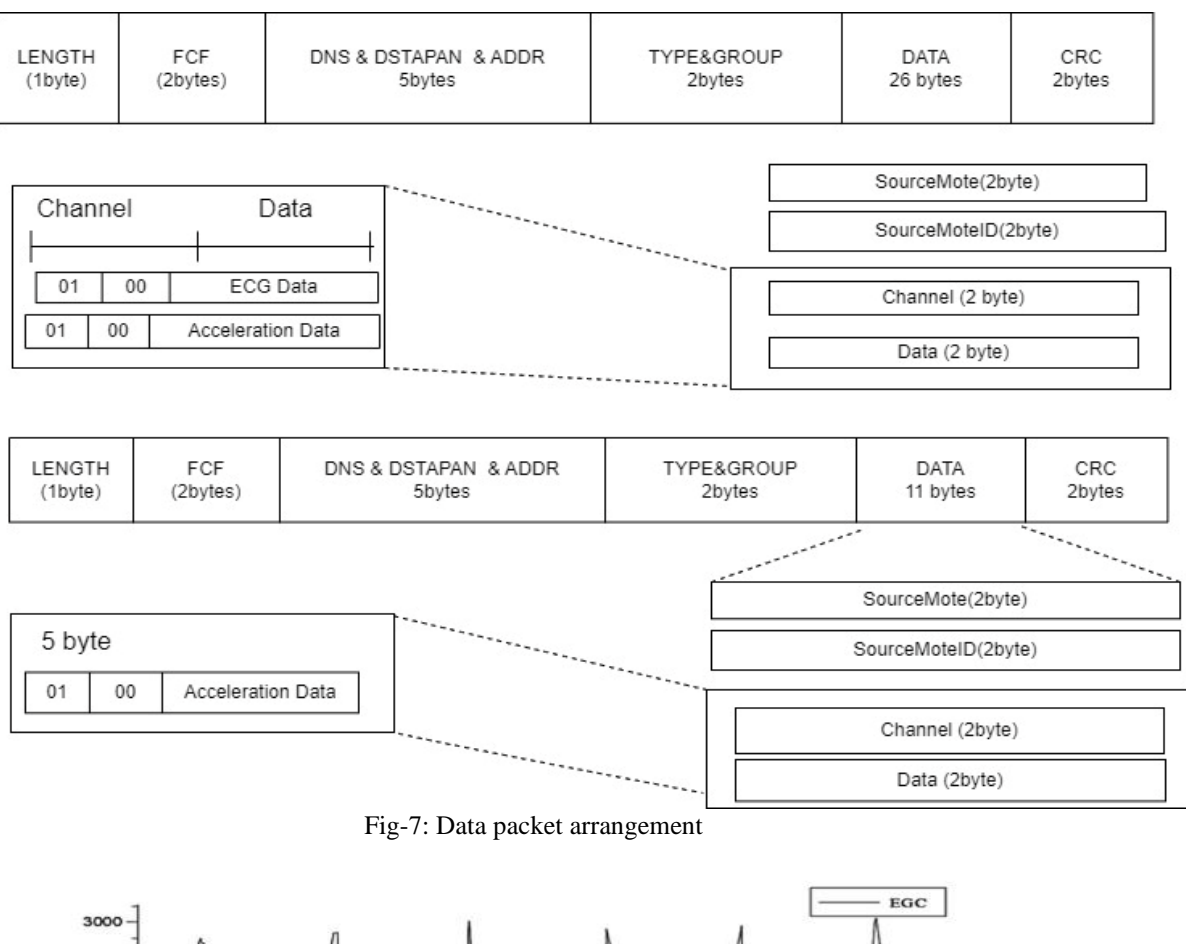
By capturing a variety of events and data, the instantaneous health observing system helps people to regularly review and monitor their health from the comfort of their own homes. An efficient way to supervise and monitor the calculated values that the sensors have recorded is made possible by the optimized database storage model. The server system of health monitoring system, measurement data like blood oxygen saturation, acceleration, and ECG are automatically stored. Physical sign trends within the system are shown in Figure 8. The system has the ability to precisely recognize and document a person's condition, even if they pass out. Furthermore, wearable technology continuously records physical sign data in day-to-day living, guaranteeing that doctors receive comprehensive data in an organized manner to facilitate accurate diagnosis.

#### 5.4 Simulation results

We exhibit our findings in this section after investigating the data features and associated disorders. In order to provide insightful information and produce quicker, more precise results, modern health observing systems make usage of real-time analysis. System performance can be slowed down by problems like unstable data supply from remote sensors and unreliable network access. In order to overcome these obstacles, we first gather a large amount of information fetching from applicable sensors. After that, we store the information in frames and a structured format. Next, we use deep learning algorithms to categorize and recognize illnesses that impact specific people. Lastly, we contrast the outcomes of various DNN designs and structures of selection.

## 5.5 Characteristics of the data

In this study, we utilize 3,214 samples, each corresponding towards a liquidate report from a clinical admission. An abstract of this data is provided in the Table 1. The study includes individuals thru 9 distinct diseases, then the data reveals that some samples are labelled with multiple phenotypes, reflecting cases where a person suffers from more than one disease. Clothing mechanisms are used towards continuously examine athletes' fitness condition data in actual information in preparing matches and competitive games to enhance the efficiency. Figure 9 illustrate the data about health of athletes measured every second. Given figure demonstrate that our suggested system effectively monitors athletes' health using real-time data collected from their wearable devices.



2500 2000 PPG 200 PPG 100 0 2 3 4 AccX AccY 2250 2000 2 Time(sec)

Fig-8: Experimental results of acceleration, ECG and PPG waveform.

# 5.6 Mean and deviation

For word-level input, the mean and standard deviation for individuals can be calculated. Once the data is is prepared, the total sample length reaches 35.95 deviations, with an average of 8.73. As shown in Table 2, the sample averages 3.80 characters and 3.40 words. The smallest sample, in terms of character count, has a mean of 0.50 and a deviation of 0.30.



Table 1: Health parameters measured from ten individuals.

No of Persons	Temp <sup>0</sup> C		BP(H/L) mmHG		O <sub>2</sub>		Heartbeat	
	A	В	A	В	A	В	A	В
1	38.2	38.1	125/92	127/89	97%	97%	78	78
2	37.2	37.4	120/80	123/81	96%	98%	80	80
3	37.5	37.6	123/89	122/90	92%	94%	85	85
4	37.2	37.2	130/91	130/92	93%	94%	85	86
5	37	37	135/90	130/90	95%	99%	78	79
6	37.7	37.8	110/90	109/83	99%	99%	79	79
7	37.4	37.3	108/83	108/84	92%	91%	81	81
8	37.3	37.3	122/92	121/90	95%	95%	82	82
9	38	38	136/95	133/95	94%	94%	75	77
10	37.5	37.5	109/84	107/82	93%	93%	89	88

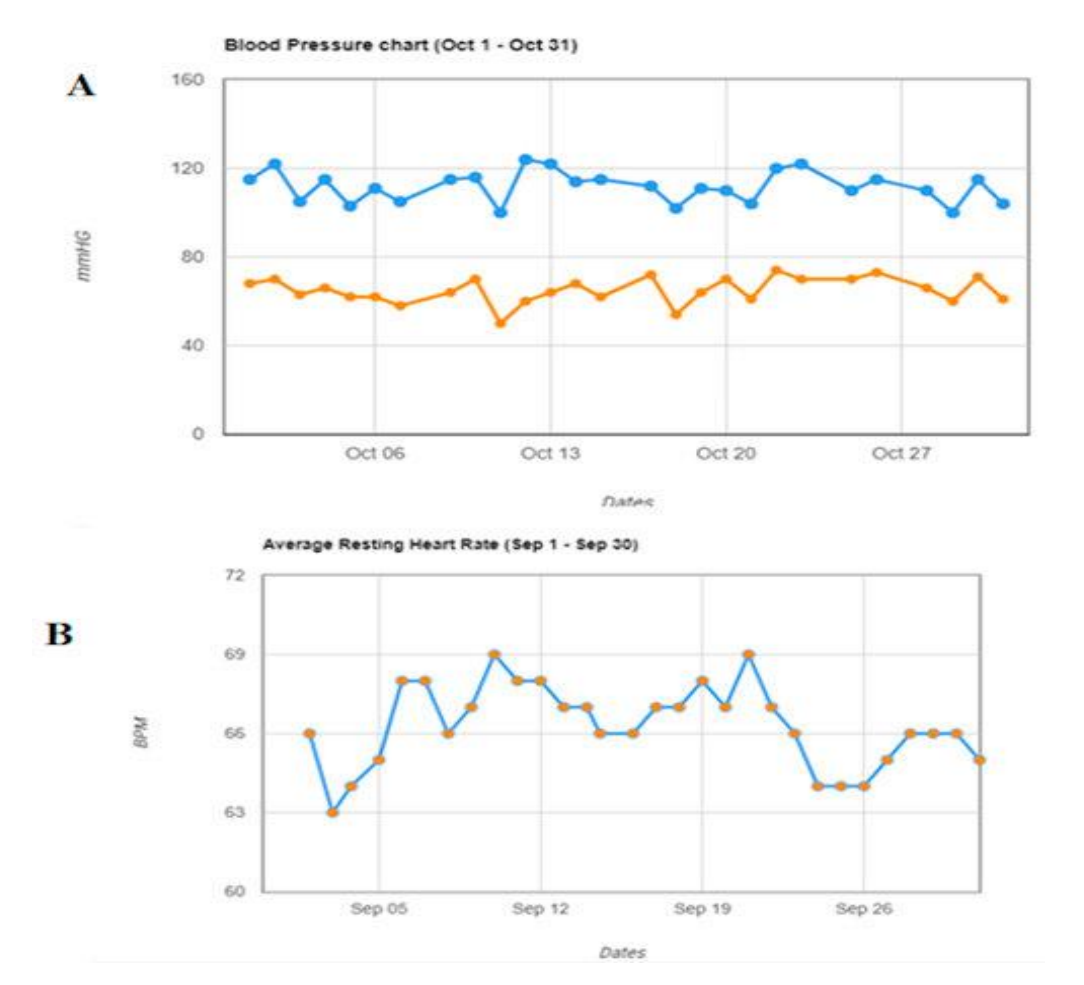


Fig 9: graphs of average Blood pressure and resting heart rate



## 5.7 Balancing classes for training

To address the perceived bias in preparing the DNN model, we employed a weight balance strategy. This involves assigning class weights to our failure features to make learning more costly. To prevent overfitting during model setup and configuration, we applied regularization techniques, such as  $L_1$  and  $L_2$  regulation and waster systems. Specifically, we used the cross-entropy failure function [45, 46] with a weight vector, where each component is

derived from a single specimen

Table 2: Attributes along with

Attribute	Mean	Deviation		
1	3.89	3.50		
2	119.80	31.00		
3	79.90	20.30		
4	21.60	17.40		
5	80.87	114.10		
6	32.11	7.89		
7	0.55	0.32		
8	22.36	34.23		
9	16.06	33.22		
10	9.89	36.77		

Standard Mean and the deviation

per class.

This approach helps the network better handle the minority class and reduce false predictions. Our methodology revealed significant differences in the results, particularly affecting the results for 2 phenotypes that are A and B, due to these balance adjustments. We employed weight balancing for our analyses to mitigate biases. Table 3 summarizes the impact of various parameters, such as activation functions and learning rate illustrating the accuracy performance across separate phenotypes. We augmented the parameter settings for every algorithm in learning to enhance efficiency. The success of the deep neural network model was evaluated using the Area under the Curve (AUC) metric, which exists commonly managed for assessing dual classification efficiency. The value of AUC changes between the 0 (low) to 1 (high), high value represents the higher classifier performance [47]. Figure 10 shows the results of different dual phenotypes using various chronological sequence making techniques. The table results show higher performance comparative to other models by the proposed deep learning model.

Table 3: Different phenotypes and their performance

Phenotypes	Percentage of Precision		Percentage of Recall		Percentage of AUC		Percentage of F1	
	A	В	A	В	A	В	A	В
Body Temp	59.66	60.8	65.44	59.44	68.55	58.9	67.67	52.34
Heartbeat	74.44	59.55	72.3	57.54	75.42	59.77	73.78	52.45
Pulse Rate	75.44	61.65	72.98	63	74.33	65.45	68.98	63.44
Blood pressure	72.33	54.55	71.91	56.44	72.5	55.54	72.44	51.34
Blood sugar	71.33	61.03	70.44	61.33	71.44	60.91	72.66	60.34
Blood glucose	68.33	59.34	68.45	58.99	73.44	63.87	71.43	60.43
ECG	72.33	56.44	70.34	56.44	71.99	65.01	70.33	59.44
EEG	73.44	59.33	72.33	60.33	74.67	60.33	74.33	58.44



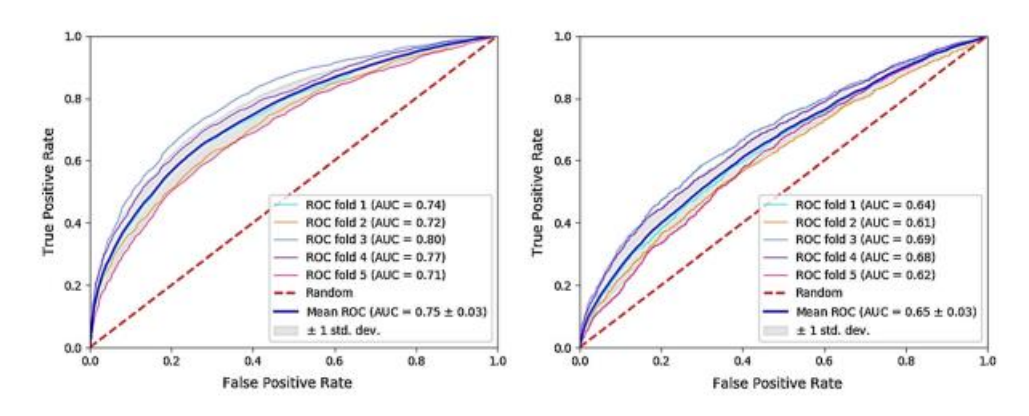


Fig.10. ROC curve of the Pulse rate and Blood sugar

8. Conclusion

In this article, the wireless sensor network with relay functionality for node of abiliment sensor device is presented. The sensors have a wireless sensor frame that is universal and designed for daily wear and ease of use. While the hand watch sensor estimates blood oxygen soaking and the chest strap sensor combines acceleration and ECG sensors. The blood oxygen saturation, acceleration, and ECG are vital signs that are thought to be essential for health monitoring. Following validation, the information gathered from these wearable sensors are routinely conserved to the real-time medical values from the athletes by this system. Furthermore, the wireless relay-enabled sensing network leads at the very less power to reduce radiation's harmful effects. Although this study's DNN model produced encouraging results, it is not without flaws.. Deeper networks can result in increased computation costs, complexity, and vanishing gradients, even though they frequently increase accuracy. Future research will tackle these issues.

**Conflict of interest:** The authors declare no conflict of interest.

# References

- [1] Liu X, He P, Chen W, Gao J. (2019) Multi-task deep neural networks for natural language understanding. arXiv doi: https://doi.org/10.18653/v1/p19-1441
- [2] Sun J, Khan F, Li J, Alshehri MD, Alturki R, Wedyan M (2021) Mutual authentication scheme for ensuring a secure device-to server communication in the internet of medical things. IEEE Internet Things J. https://doi.org/10.1109/JIOT.2021.3078702.
- [3] M. S. Obaidat and P. Nicopolitidis, Smart Cities and Homes: Key Enabling Technologies. Amsterdam, The Netherlands: Elsevier, 2016.
- [4] A. H. Sodhro, L. Zongwei, S. Pirbhulal, A. K. Sangaiah, S. Lohano, and G. H. Sodhro, "Power-management strategies for medical information transmission in wireless body sensor networks," IEEE Consum. Electron. Mag., vol. 9, no. 2, pp. 47–51, Mar. 2020.
- [5] R. Cheour, F. Derbel, O. Kanoun, and M. Abid, "Wireless sensor networks with power management for low energy consumption," in Proc. 10th Int. Multi-Conf. Syst., Signals Devices (SSD), Mar. 2013, pp. 1–6.
- [6] Miao Yu, Quan T, Qinglong Peng XY, Liu L (2021) A model based collaborate filtering algorithm based on stacked autoencoder. Neural Comput Appl. https://doi.org/10.1007/s00521-021-05933-8 22. Zhou G-P, Chen D, Liao S, Huang R-B (2015).
- [7] T. S. P. See, Y. Ge, T. M. Chiam, J.W. Kwan, and C. W. Kim, "Experimental correlation of path loss with system performance in WBAN for healthcare applications," in Proc. IEEE 13th Int. Conf. E-Health Netw., Appl. Services, Jun. 2011, pp. 221–224.

- [8] A. H. Sodhro, S. Pirbhulal, G. H. Sodhro, A. Gurtov, M. Muzammal, and Z. Luo, "A joint transmission power control and duty-cycle approach for smart healthcare system," IEEE Sensors J., vol. 19, no. 19, pp. 8479–8486, Oct. 2019.
- [9] G. Miao, N. Himayat, Y. Li, and A. Swami, "Cross-layer optimization for energy-efficient wireless communications: A survey," Wireless Commun. Mobile Comput., vol. 9, no. 4, pp. 529–542, Apr. 2009.
- [10] S. Xiao, A. Dhamdhere, V. Sivaraman, and A. Burdett, "Transmission power control in body area sensor networks for healthcare monitoring," IEEE J. Sel. Areas Commun., vol. 27, no. 1, pp. 37–48, Jan. 2009.
- [11] A. H. Sodhro, S. Pirbhulal, M. Qaraqe, S. Lohano, G. H. Sodhro, and N. U. R. Junejo, and Z. Luo, "Power control algorithms for media transmission in remote healthcare systems," IEEE Access, vol. 6, pp. 42384–42393, 2018.
- [12] A. H. Sodhro, L. Zongwei, S. Pirbhulal, A. K. Sangaiah, S. Lohano, and G. H. Sodhro, "Power-management strategies for medical information transmission in wireless body sensor networks," IEEE Consum. Electron. Mag., vol. 9, no. 2, pp. 47–51, Mar. 2020.
- [13] M. Muzammal, R. Talat, A. H. Sodhro, and S. Pirbhulal, "A multi-sensor data fusion enabled ensemble approach for medical data from body sensor networks," Inf. Fusion, vol. 53, pp. 155–164, Jan. 2020.
- [14] K. W. Choi and D. I. Kim, "Stochastic optimal control for wireless powered communication networks," IEEE Trans. Wireless Commun., vol. 15, no. 1, pp. 686–698, Jan. 2016.
- [15] C. Yi, L. Wang, and Y. Li, "Energy efficient transmission approach for WBAN based on threshold distance," IEEE Sensors J., vol. 15, no. 9, pp. 5133–5141, Sep. 2015.
- [16] S. Tanwar, P. Patel, K. Patel, S. Tyagi, N. Kumar, and M. S. Obaidat, "An advanced Internet of Thing based security alert system for smart home," in Proc. IEEE Int. Conf. Comput., Inf. Telecommun. Syst. (CITS), Dalian, China, Jul. 2017, pp. 25–29.
- [17] Y. H. Ugur, "Transmission power control for link-level handshaking in WSNs," IEEE Sensor J., vol. 16, no. 2, pp. 561–576, Jan. 2016.
- [18]. Tanwar, P. Patel, K. Patel, S. Tyagi, N. Kumar, and M. S. Obaidat, "An advanced Internet of Thing based security alert system for smart home," in Proc. IEEE Int. Conf. Comput., Inf. Telecommun. Syst. (CITS), Dalian, China, Jul. 2017, pp. 25–29.
- [19] S. K. Baliarsingh, S. Vipsita, K. Muhammad, and S. Bakshi, "Analysis of high-dimensional biomedical data using an evolutionary multi-objective emperor penguin optimizer," Swarm Evol. Comput., vol. 48, pp. 262–273, Aug. 2019.
- [20] T. Wu, F. Wu, J.-M. Redoute, and M. R. Yuce, "An autonomous wireless body area network implementation towards IoT connected healthcare applications," IEEE Access, vol. 5, pp. 11413–11422, 2017.
- [21] N. N. Hurrah, S. A. Parah, J. A. Sheikh, F. Al-Turjman, and K. Muhammad, "Secure data transmission framework for confidentiality in IoTs," Ad Hoc Netw., vol. 95, Dec. 2019, Art. no. 101989.
- [22] S. Pirbhulal, H. Zhang, M. E. Alahi, H. Ghayvat, S. Mukhopadhyay, Y.-T. Zhang, and W. Wu, "A novel secure IoT-based smart home automation system using a wireless sensor network," Sensors, vol. 17, no. 12, p. 69, 2016.
- [23] NICTA. Accessed: Aug. 29, 2019. [Online]. Available: http://www.nicta.com.au.
- [24] M. A. G. Santos, R. Munoz, R. Olivares, P. P. R. Filho, J. D. Ser, and V. H. C. D. Albuquerque, "Online heart monitoring systems on the Internet of health things environments: A survey, a reference model and an outlook," Inf. Fusion, vol. 53, pp. 222–239, Jan. 2020.
- [25] R. M. Sarmento, F. F. X. Vasconcelos, P. P. R. Filho, and V. H. C. de Albuquerque, "An IoT platform for the analysis of brain CT images based on Parzen analysis," Future Gener. Comput. Syst., vol. 105, pp. 135–147, Apr. 2020.
- [26] T. Han, L. Zhang, S. Pirbhulal, W. Wu, and V. H. C. de Albuquerque, "A novel cluster head selection technique for edge-computing based IoMT systems," Comput. Netw., vol. 158, pp. 114–122, Jul. 2019.
- [27] C. Taramasco, T. Rodenas, F. Martinez, P. Fuentes, R. Munoz, R. Olivares, V. H. C. De Albuquerque, and J. Demongeot, "A novel monitoring system for fall detection in older people," IEEE Access, vol. 6, pp. 43563–43574, 2018.
- [28] Zhang Q, Yang LT, Chen Z, Li P (2017) An improved deep computation model based on canonical polyadic decomposition. IEEE Trans Syst Man Cybern Syst 48(10):1657–1666



- [29] Jan MA, Khan F, Khan R, Watters P, Alazab M, Rehman AU (2021) A lightweight mutual authentication approach for intelligent wearable devices in health-CPS. IEEE Trans Ind Inf 17(8):5829–5839
- [30] Wu Y, Tan H, Qin L, Ran B, Jiang Z (2018) A hybrid deep learning-based traffic flow prediction method and its understanding. Transp Res Part C Emerg Technol 90:166–180. https://doi.org/10.1016/j.trc.2018.03.001
- [31] Xu Yu, Zhan D, Liu L, Lv H, Lingwei Xu, Junwei Du (2021) A privacy-preserving cross-domain healthcare wearables recommendation algorithm based on domain-dependent and domain independent feature fusion. IEEE J Biomed Health Inform. https://doi.org/10.1109/JBHI.2021.3069629
- [32] M. M. E. Mahmoud, J. J. P. C. Rodrigues, S. H. Ahmed, S. C. Shah, J. F. Al-Muhtadi, V. V. Korotaev, and V. H. C. De Albuquerque, "Enabling technologies on cloud of things for smart healthcare," IEEE Access, vol. 6, pp. 31950–31967, 2018.
- [33] Miao JH, Miao KH (2018) Cardiotocographic diagnosis of fetal health based on multiclass morphologic pattern predictions using deep learning classification. Int J Adv Comput Sci Appl 9:1–11. https://doi.org/10.14569/IJACSA.2018.090501.
- [34] Smith L (1988) A tutorial on principal components analysis. Commun Stat Theory Methods 17:3157–3175
- [35] Sindi H, Nour M, Rawa M, O" ztu"rk S, Polat K (2021) A novel hybrid deep learning approach including combination of 1D power signals and 2D signal images for power quality disturbance classification. Expert Syst Appl 174:114785
- [36] Shahamat H, Abadeh MS (2020) Brain MRI analysis using a deep learning based evolutionary approach. Neural Netw 126:218–234
- [37] Fang C, Moriwaki Y, Li C, Shimizu K (2019) Prediction of antifungal peptides by deep learning with character embedding. IPSJ Trans Bioinf 12:21–29
- [38] Chou K-C (2010) Graphic rule for drug metabolism systems. Curr Drug Metab 11:369–378. https://doi.org/10.2174/138920010791514261
- [39] Wong TT, Yang NY (2017) Dependency analysis of accuracy estimates in k-fold cross-validation. IEEE Trans Knowl Data Eng 29:2417–2427. https://doi.org/10.1109/TKDE.2017.2740926
- [40] Liu G, Liu J, Cui X, Cai L (2012) Sequence-dependent prediction of recombination hotspots in Saccharomyces cerevisiae. J Theor Biol 293:49–54. https://doi.org/10.1016/j.jtbi.2011.10.004